Energy, exergy and thermoeconomic analysis of an industrial solar pond

M. Montalà[1,2], K. Ganesan[1,2], O. Casal[1,2], J.L. Cortina[2,3], M. Santarelli[4], C. Valderrama[1,2,3,*]

[1] Barcelona School of Industrial Engineering, ETSEIB, UPC•BarcelonaTECH

[2] Chemical Engineering Department, UPC•BarcelonaTECH

[3] Barcelona Research Center for Multiscale Science and Engineering, 08930 Barcelona, Spain

[4] Department of Energy, Politecnico di Torino, C.so Duca Degli Abruzzi 24, Turin, 10129, Italy

*Correspondence should be addressed to: César Valderrama

Departament d'Enginyeria Química, Universitat Politècnica de Catalunya-Barcelona TECH

C/ Eduard Maristany, 10-14 (Campus Diagonal-Besòs), 08930 Barcelona, Spain

Tel.: 93 4011818

Email: cesar.alberto.valderrama@upc.edu

Abstract

This study evaluates the viability of an industrial salinity gradient solar pond during two operating seasons (2014 and 2015). The Granada solar pond was built to supply low-temperature heat (up to 60°C) to satisfy the temperature requirements of the flotation unit in a mineral processing plant (Solvay Minerales in Granada (Spain)). Energy analysis indicates that the non-convective zone (NCZ) and the upper convective zone (UCZ) have low efficiencies because these zones have a low capacity to store heat, and no heat extractions are carried out from these zones. In contrast, heat extraction in the lower convective zone (LCZ) has a positive impact on the system because it increases the capacity of the solar pond to store energy. Higher efficiencies were achieved in the second operation period in the LCZ, since higher amount of heat was extracted during this period. The overall exergy efficiency of the LCZ after the first and second operation periods was 1.6% and 2.3%, respectively. The solar pond works at temperatures

close to room temperature and thus the exergetic efficiency decreases significantly. Regarding the thermoeconomic analysis, the cost of exergy stored is studied in this work, using two different approaches, by estimating the minimum price for exergy stored or the minimum surface area that ensure the thermoeconomic viability. The price of the stored exergy tends to decrease inversely to the price of fuel oil. Thus, the cost of the stored exergy must be four to five times higher than the price of fuel oil for the solar pond system to be feasible. On the other hand, solar pond technology is affected by economies of scale; the larger the solar pond, the higher the inflation rates and the lower the cost reduction rates that can be accommodated. This implies that estimating the cost of the stored exergy is complex due to the variability of the processes involved and can lead to erroneous interpretations when evaluating the viability of a solar pond from a thermoeconomic perspective.

Keywords: Solar energy; energy storage; salinity gradient solar pond; mineral processing; flotation unit

Nomenclature

Parameters		**Greek Symbols**	
I	Solar radiation	θ_i	Angle of incidence
Q	Energy flux	θ_r	Refraction angle
$E/\dot{E}$	Exergy flux	$\emptyset$	Latitude
$\dot{Z}$	Annual capital cost	δ	Declination angle of the sun
$Q_{stored_{layer}}$	Energy stored in a certain layer	ω	Hour angle
$E_{stored_{layer}}$	Exergy stored in a certain layer	λ	Reflectivity of the bottom of the solar pond
$Q_{in_{layer}}$	Input energy in a certain layer	η	Energy efficiency
$E_{in_{layer}}$	Input exergy in a certain layer	ψ	Exergy efficiency
$Q_{out_{layer}}$	Output energy in a certain layer	α	Thermal expansion coefficient
$E_{out_{layer}}$	Output exergy in a certain layer	β	Salinity expansion coefficient

$Q_{s_{out}}$	Outlet solar radiation inlet	M	Aggregated exergy fluxes
$E_{s_{in}}$	Inlet solar radiation exergy	**Subscripts**	
$E_{s_{out}}$	Outlet solar radiation exergy	i	Layer
$Q_{abs_{layer}}$	Energy absorbed by a layer	t	Time
$E_{abs_{layer}}$	Exergy absorbed by a layer	B	Bottom
$Q_{in_{layer \rightarrow layer}}$	Energy transmitted from one layer to another	T	Net Temperature
$E_{in_{layer \rightarrow layer}}$	Exergy transmitted from one layer to another	CI	Investment cost
Q_{ext}	Energy extracted from the system	OM	Operation & Maintenance Cost
E_{ext}	Exergy extracted from the system	ch	Chemical
$Q_{loss_{layer}}$	Energy lost from a certain layer	ph	Physical
$E_{useless_{layer}}$	Exergy lost and destroyed in a certain layer	**Abbreviations**	
c_{ext}	Cost of the extracted exergy flux	$SGSP$	Salinity Gradient Solar Pond
c_{stored}	Cost of the stored exergy	SP	Solar Pond
c_{solar}	Cost of the solar exergy	UCZ	Upper convective zone
m_{layer}	Water mass of a certain layer	NCZ	Non convective zone
Cp_{layer}	Heat capacity of a certain layer	LCZ	Lower convective zone
T_{layer}	Temperature of a certain layer	Fr	Froude number
$\dot{m}_{ext}$	Mass flow rate through the heat exchanger to extract heat	$CAPEX$	Capital expenditures
Cp	Heat capacity of water used to extract heat	$OPEX$	Operating expense

T_{in}	Water temperature before the heat exchanger	$LSTM$	Local Standard Time Meridian
T_{ext}	Water temperature after the heat exchanger	LT	Local Time
R	Fraction of the solar radiation directly reflected to the environment	GMT	Greenwich Mean Time
L	Total depth of the solar pond	EoT	Equation of Time
R_{cond}	Conductive resistance	TCF	Time correction factor
Δz	Thickness of contact zone	LST	Local Solar Time
A	Area		
K	Thermal conductivity		
E	Static stability		
i_r	Economy inflation		
n_y	Lifetime of the solar pond		
$Inv.Cost$	Investment cost of the solar pond		
x_i	Molar fraction		
$e^0_{x,ch}$	Standard molar chemical exergy		
Cp	Heat capacity of water used to extract heat		

1. Introduction

Solar energy is an abundant, clean and inexhaustible source of energy that can reduce the impact of the climate crisis caused by the use of fossil fuels. However, the use of solar thermal energy is associated with significant challenges due to its low energy density and its intermittent characteristics. The salinity gradient solar pond technology provides a solution using a large area of land that allows energy to be

collected and stored [1, 2]. A solar pond is a system capable of storing part of the received solar radiation for a long period of time and providing heat to an external system.

The salinity gradient solar pond (SGSP) system generally consists of three zones, namely the upper convective zone (UCZ), non-convective zone (NCZ) and lower convective zone (LCZ). The UCZ, which is the thinnest layer, has a temperature close to room temperature and possesses the lowest salinity concentration (5–10%). The middle zone of the SGSP is called the NCZ or gradient zone, where the temperature and the degree of salinity increase with depth. The salinity gradient in the NCZ provides a transparent insulating layer under various climatic conditions to store solar energy at the bottom of the pond [3]. The LCZ is the storage zone, which has the highest salinity concentration (15–30%) [4].

The efficiency of solar ponds is low due to the lack of retention of solar radiation that is absorbed by the lower convective zone, which is the main reservoir for stored energy in solar ponds [4]. The thermal efficiency of solar ponds has been commonly defined and evaluated based on their energy storage capacity or the quantum of heat extracted from them. It is worth mentioning that the operation of the solar pond is a continuous process of charging, storage and discharge [5] [6]. For heat extraction from solar ponds, there are two methods [7]: first is to circulate hot LCZ water through an external heat exchanger, and second is to install heat exchangers within the LCZ through which a suitable working fluid flows [8]. An appreciable portion of heat energy stored inside the lower convective zone (LCZ) gets conducted to the ground below as waste, which can be recovered by installing heat exchangers inside the ground can enhance the output of solar ponds quite significantly [9].

The amount of heat extraction from the solar pond depends on the level of demand for the heating process, which implies that the amount of energy extracted can be greater or less than the energy stored in the solar pond. During certain periods, there may be no heat extraction, which doesn't mean that the efficiency of the solar pond can be assigned as zero. This is because the absorbed energy is still being stored by the pond during this period [10]. The unused part of the available energy undergoes a quality degradation termed exergy destruction that causes the system to deviate from its expected ideal

operating state. Verma and Das [11] reported that the rate of exergy destruction caused by the operation of the pond (heat extraction) is underestimated by the assumption of an infinite heat transfer coefficient that does not affect the stability of the pond. For instance, the energy available in a system that has reached an equilibrium with its surroundings is no longer suitable for use. Furthermore, the exergetic analysis preserves the energy conservation principle by introducing the quality degradation of energy caused by the entropy generation in real system transformations [12] [13]. Different authors have suggested theoretical models or lab scale analysis to study both the energy and exergetic performance of solar pond technology [14]. Bozkurt and Karakilcik [15] evaluated the exergetic performance of a cylindrical solar pond (1.6 m of diameter) integrated with four flat plate collectors. Authors concluded that exergy analysis allows to identify the heat losses and to improve the performance of the system. The influence of the geometry on the solar pond performance was also evaluated from the exergy perspective by Dehghan et al. [16]. Two small solar ponds (square and circular cross sections) with a surface area of 3 m^2 were evaluated using the experimental data collected during 10 months. The energy and exergy efficiency reported for circular solar pond were higher than for square solar pond at the LCZ. Authors concluded that storage capacity is higher in the circular solar pond.

The influence of shading walls on storage capacity of small solar pond (4 m^2 circular and square cross-section) was evaluated by Khalilian [17, 18]. Numerical analysis of energy and exergy efficiencies was carried out by author considering the shadows effect and concluded that exergy efficiency was one order of magnitude lower than the energy efficiency. Njoku et al. [19] critically reviewed the aforementioned studies, highlighting that the temperature stratifications in the NCZ were not accounted for when calculating the exergies, using the average temperatures of the gradient leading to significant errors in the computed exergies. A 1-D transient numerical model was proposed, including temperature stratification within the SGSP as well as heat extraction from the LCZ. Authors concluded that the largest exergy destructions occurred in the LCZ. Therefore it was suggested that in formulating measures for enhancing SGSP performance. Heat extraction process was also evaluated in terms of transient thermal

performance of solar pond. Extraction at different rates at the LCZ and at the NCZ were considered as well as simultaneous extraction from both zones using a finite difference method. Results indicated that maximum exergy efficiency was obtained extracting heat from the LCZ only [20]. Recently, Cardoso et al. [21] reported a numerical analysis of the potential performance of a 1 ha solar pond located on Caota Beach, in Benguela, Angola. Authors concluded that heat losses at the LCZ penalize the useful energy extracted from this zone and lead to a very low energy and exergy efficiencies of the pond.

Namin et al. [22] described the potential of solar pond technology in recent years, despite the low exergetic efficiency of a SGSP due to the immense irreversibilities in all regions of the system, when integrated with hybrid energy systems (especially in systems power and desalination). It is worth to mention the evaluation of construction of SGSP refrigeration system [23], the enhanced design of a large scale SGSP power plant using ORC systems and two-phase closed thermosyphons to generate electricity [24, 25], the hydrogen production by flat-plate collectors assisted by a solar pond [26], the feasibility design of a SGSP- humidification–dehumidification desalination system for producing freshwater [4, 27]. In most of aforementioned studies [20-27] the solar pond formulation is simplified to the heat collection efficiency assuming mathematical relations obtained in previous studies. Only the study by Zeynali et al [28], when evaluating the power generation using organic Rankine cycles (ORC) and trilateral modified flash cycles (TFC) assisted by a solar pond, reported a detailed description of each zone, however, how the temperature of the gradient is considered in NCZ analysis is not mentioned.

To the best of our knowledge, the performance evaluation of industrial solar ponds using energy and exergy analysis has not been reported. The present study evaluates the efficiency of a 500 m^2 industrial solar pond built in Spain to supply heat to a flotation unit in a mine facility. Energy and exergetic efficiencies are detailed analysed for each zone of the solar pond and the overall efficiencies of the system are estimated. Finally, a thermoeconomic analysis is also performed in order to assess the feasibility of the Granada solar by quantifying the cost of the exergy stored in the solar pond during two operating seasons.

2. Materials and Methods

2.1 Description of the Granada solar pond

The solar pond was constructed in the Solvay Minerales facilities in Granada (South Spain) in 2014. Details of the design, construction and operation were reported in Alcaraz et al. [3]. The solar pond was installed in a mine facility producing celestine ($SrSO_4(s)$). The processed rock, with a celestine content of 30–50%, is milled and then concentrated up to a content of 90% by using a flotation stage. The solar pond was constructed to deliver the heat needed to preheat the water (> 60 °C) used in the mineral flotation unit. The total area of the pond is 500 m^2 (20 × 25 m) and it has a depth of 2.2 m. The LCZ was designed to be 0.6 m thick, the NCZ was 1.4 m thick, and the UCZ was 0.2 m thick. The main climatological parameters of the solar pond's location [29] are listed in Table 2.

Table 1. Location and climatological parameters at Solvay Minerales mining facilities in Granada (Spain).

Coordinates			37° 3' 0" N, 3° 45' 0" W									
Altitude (m)			929									
Wind average speed (m/s)			2.3									
Summer maxim temperature (°C)			33.0									
Winter minimal temperature (°C)			-7.0									
	January	February	March	April	May	June	July	August	September	October	November	December
Average	3.10	4.20	7.30	10.0	13.3	18.1	21.9	21.4	18.0	12.0	7.2	4.1
Solar radiation	283	346	496	618	734	813	838	748	565	400	275	227

Table 1. Location and weather parameters at the Solvay Minerales facilities (Granada, Spain).

The bottom and the walls were insulated using a synthetic insulation material, ChovAFOAM 300-M50 (thermal conductivity = 0.034 W/mK; thickness = 50 mm; maximum pressure = 300 kPa; maximum temperature = 65 °C) in order to prevent heat losses. Expanded clay pellets (Arlita) were laid on the base of the pond to a total height of 50 mm. The remainder of the wall, not covered with Arlita, was laid with a geotextile (non-woven polyester GTXnw PS NTL, Atarfil, Spain). In addition, a secondary (PE) liner was used to prevent 1 leakage in the system (thickness = 2 mm).

To control the stability of the salinity gradient, samples are taken every 10 cm from the bottom area through a PVC pipe (6 mm in diameter with a height of 3 m) to determine the density, pH, and turbidity

of the system over its entire height. A DMA 35 portable density meter (Anton Par; accuracy of ±0.001 g/cm3) is used to measure the density. The pH and turbidity are measured by a portable pH meter (Crison pH25, accuracy of ±0.01 pH) and a portable turbidity meter (Hanna HI93703C, accuracy of ±0.5 NTU), respectively. The temperature measurement at different heights is performed by 42 sensors (thermo-resistances, PT100 type, Abco, Spain) uniformly distributed at intervals of 5 cm, starting 0.5 cm from the bottom and installed in plastic supports. The temperature is measured every 2 s and the average after 10 min as well as the hourly and daily average is recorded. The monthly average temperature of each zone is determined by averaging the values recorded daily. The weather parameters are measured by means of an automatic weather station, the CR1000 Measurement and Control System (Campbell Scientific, Barcelona, Spain).

Before the installation of the solar pond, water was heated using a boiler fed with gasoil. After starting its operation, a degradation in the salinity gradient was detected through monitoring the density profile, and in April 2015 the salinity gradient was considered technically destroyed. In September 2015 the solar pond was refilled and its operation restarted. No problems were detected until April 2016 when the salinity gradient started to deteriorate again. In this study, energy and exergy analyses are detailed for the two operation seasons.

2.2 Energy analysis

In this section, all the energy fluxes found in the system are detailed as depicted in Figure 1.

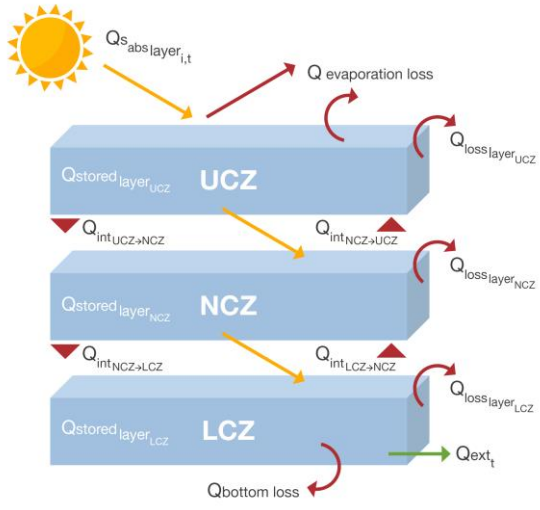

a

b

Figure 1. a) Schematic description of energy fluxes and b) view of the 500 m^2 solar pond at Solvay Minerales facilities (Granada, Spain).

As mentioned earlier, a solar pond is a system that allows the storage of heat, which is provided to an external application. Hence, the amount of energy stored can be determined as the difference between all the input and output energy fluxes (Eq. 1).

$$Q_{stored_{layer_i}} = \sum_{0}^{t} Q_{in_{layer_{i,t}}} - \sum_{0}^{t} Q_{out_{layer_{i,t}}} \quad (1)$$

where $Q_{in_{layer_{i,t}}}$ is composed of the solar radiation absorbed by the layer ($Q_{S_{abs}layer_{i,t}}$) and the heat transferred from the lower or/and upper layers ($Q_{int_{layer_{i,t} \rightarrow layer_{i+1,t}}}$). $Q_{out_{layer_{i,t}}}$ is composed of the heat transferred to the lower and/or upper layers ($Q_{int_{layer_{i+1,t} \rightarrow layer_{i,t}}}$), the heat extracted from the system (Q_{ext_t}) and the heat lost ($Q_{loss_{layer_{i,t}}}$).

The heat stored in each zone during a certain period may be obtained by comparing the temperature at the beginning of the period with the temperature at the end according to Eq. 2.

$$Q_{stored_{layer_{i,t}}} = mass_{layer_i} \cdot Cp_{layer_i} \cdot (T_{layer_{i,t}} - T_{layer_{i,t-1}}) \quad (2)$$

where $T_{layer_{i,t}}$ is the temperature of the layer at the end of the period, $T_{layer_{i,t-1}}$ is the temperature of the layer at the beginning, Cp_{layer_i} is the water heat capacity and $mass_{layer_i}$ is the total mass of the zone.

The $Q_{stored_{layer_{i,t}}}$ in the LCZ and UCZ can be determined using the average temperature of the zones because there are small temperature variations in these two zones. However, in the NCZ the presence of the temperature gradient results in significant variation in temperature values from one sensor to another. Hence, the NCZ should be divided into different sub-layers and the energy stored in each sub-layer independently determined. At the end, the energy stored in the NCZ is the sum of the energy stored in all the sub-layers.

Part of the incident solar radiation that arrives to the solar pond surface is directly reflected, i.e. part of the solar radiation never enters the system. The fraction of the solar radiation that remains after the reflection can be determined according to Eq. 3:

$$I_{o_t} = I_t(1 - R_t) \quad (3)$$

where I_{o_t} is the amount of solar radiation penetrating the solar pond, I_t is the total amount of solar radiation that arrives at the solar pond surface and is measured by the sensors of the meteorological station and R_t is the fraction of the solar radiation directly reflected to the environment. The description of the equations used to determine the solar radiation at each layer of the SP using the Bryant and Colbeck method [30] is reported in Section 1 of the Supplementary Material.

The input energy to each layer coming from solar radiation is the result of multiplying the net solar radiation at the depth of the layer (I_{xT}) by the area of the layer (A) (Eq. 4):

$$\mathrm{Q_{s_{in_{i,t}}}} = I_{xT_{i,t}} \cdot A_i \quad (4)$$

Solar radiation is considered as an input. However, $\mathrm{Q_{s_{in}}}$ represents the amount of energy that arrives at each layer. Part of this energy is transmitted to the layer immediately below. Hence, there is a solar radiation input and output flux. To consider solar radiation only as input flux, the concept of absorbed energy is suggested, which balances the input and output fluxes of solar radiation in each layer (Eq. 5):

$$Q_{S_{abs}\,layer_{i,t}} = Q_{S_{in}\,layer_{i,t}} - Q_{S_{in}\,layer_{i+1,t}} \quad (5)$$

The different zones of the system in contact with each other have different temperature characteristics. As a result, part of the heat is transmitted from the higher temperature layer to the lower temperature layer. Typically, the heat is transferred from the LCZ to the NCZ and from the NCZ to the UCZ. However, in some periods these heat fluxes can be reversed.

These internal heat fluxes are mostly transmitted by conduction and may be determined through Eq. 6 [31]:

$$Q_{int_{layer_{i,t} \rightarrow layer_{i+1,t}}} = \frac{T_{i,t} - T_{i+1,t}}{R_{cond_{i \rightarrow i+1,t}}} \quad (6)$$

In Eq. 6, it is assumed that the heat fluxes are transferred from layer (i) to layer $(i+1)$. A negative result would indicate the opposite heat transfer. T_i is the temperature measured by the sensor of the heat emitter zone closest to the nearest heat receptor, T_{i+1} is the temperature measured by the sensor of the heat receptor zone closest to the heat emitter and $R_{cond_{i \rightarrow i+1}}$ is the conductive resistance, which can be determined by Eq. 7:

$$R_{cond_{i,t}} = \frac{\Delta z}{A_i \cdot k_{i,t}} \quad (7)$$

where Δz is the thickness of the contact zone, i.e. the height difference of the sensors used in the temperature measurements, A is the area of the contact zone and k is the thermal conductivity. Thermal conductivity is defined in Eq. 8 [32], relating the temperature in the contact zone (T), the composition of the water (m), and optimal coefficients (a). The composition of the water is proportional to the salinity $S_{i,t}$ of the solar pond as indicated in Eq. 9.

$$k_{i,t} = \sum_{i=0}^{2} \left[\left(\sum_{j=0}^{2} a_{ij} T_{i,t}^{j} \right) m^{i} \right] \quad (8)$$

$$m_{i,t} = \frac{S_{i,t} \cdot 1000}{\frac{54{,}44}{(1 - S_{i,t})}} \quad (9)$$

The heat extracted from the solar pond is an output energy flux only found in the LCZ. The amount of heat extracted may be determined through Eq. 10:

$$Q_{ext_t} = \dot{m}_{ext_t} \cdot Cp \cdot \left(T_{ext_t} - T_{in_t} \right) * Time \quad (10)$$

where $\dot{m}_{ext}$ is the mass flow rate of the extractions directly measured, Cp is the water heat capacity, T_{ext} is the water temperature at the exit of the solar pond heat exchanger, T_{in} is the water temperature at the inlet of the heat exchanger and $Time$ the period in seconds during which heat is extracted from the system.

Additionally, part of the energy that arrives in the system is lost in different ways. Energy losses are found in the bottom, walls, surface etc. Due to the difficulty in determining each type of loss, all of them are considered in a single variable determined as the difference between all the energy input fluxes to the zone, all the energy output fluxes from the zone and the energy stored in the zone (Eq. 11):

$$Q_{loss_{layer_i}} = \sum_{0}^{t}\left[Q_{S_{abs}layer_{i,t}} + Q_{int_{layer_{i+1,t}\rightarrow layer_{i.t}}} + Q_{int_{layer_{i-1,t}\rightarrow layer_{i,t}}}\right] - \sum_{0}^{t}\left[Q_{int_{layer_{i,t}\rightarrow layer_{i+1,t}}} + Q_{int_{layer_i,\mathrm{t}\rightarrow layer_{i+1,t}}} + Q_{stored_{layer_{i,t}}}\left(+Q_{ext_t}\right)\right] \quad (11)$$

2.3 Exergy analysis

Energy does not provide information about the quality of the energy, but exergy analysis may overcome this shortcoming. As in energy analysis, the exergy stored at the end of one period is the difference between all the input and output exergy fluxes (Eq. 12).

$$E_{stored_{layer_i}} = \sum_{0}^{t} E_{in_{layer_{i,t}}} - \sum_{0}^{t} E_{out_{layer_{i,t}}} \quad (12)$$

$E_{in_{layer_i}}$ is composed of the exergy of the solar radiation absorbed by the layer ($E_{S_{abs}layer_i}$) and the exergy transferred from the lower or/and upper layers ($E_{int_{layer_i\rightarrow layer_{i+1}}}$). $E_{out_{layer_i}}$ is composed of the exergy transferred to the lower and/or upper layers ($E_{int_{layer_{i+1}\rightarrow layer_i}}$), the exergy extracted from the system (E_{ext}), the exergy losses ($E_{loss_{layer_i}}$) and the exergy destroyed ($E_{destroyed_{layer_i}}$).

The exergy stored in each layer can also be determined according to Eq. 13:

$$E_{stored_{layer_{i,t}}} = \mathrm{e_{ph}} + e_{ch}$$
$$= mass_{layer_i} \cdot Cp_{layer_i}$$
$$\cdot \left((T_{layer_{i,t}} - T_{layer_{i,t-1}}) - \left(T_{0_t} \ln\left(\frac{T_{layer_{i,t}}}{T_{layer_{i,t-1}}}\right) \right) \right) + x_i \cdot e^0_{x,ch} \quad (13)$$
$$+ R \cdot T_0 \cdot x_i \ln(x_i)$$

The exergy stored is composed of the physical exergy ($\mathrm{e_{ph}}$) and the chemical exergy (e_{ch}). According to Date et al. [33], the chemical exergy has much less influence than the physical exergy because there are no chemical reactions and the chemical changes are relatively small. Therefore, studies reported on solar ponds exclude chemical exergy in their analysis. However, in order to provide a more accurate analysis, chemical exergy is also included in this study based on Date et al. [33].

In Eq. 13, x_i is the molar fraction of the solute (NaCl), $e^0_{x,ch}$ is the standard molar chemical exergy of the NaCl, obtained from [34], and R is the universal gas constant. As in energy analysis, while the $E_{stored_{layer_i}}$ in the LCZ and UCZ may be determined using average values, the NCZ should be divided into different sub-layers due to the temperature gradient.

The solar radiation energy flux is a radiative energy, and the exergy associated with radiative heat fluxes can be defined by Eq. 14, where the coefficients are as a result of Stefan–Boltzmann law [35]:

$$E_{S_{abs}\,layer_{i,t}} = Q_{S_{abs}\,layer_{i,t}} \left(1 - \frac{4}{3}\left(\frac{T_{0_t}}{T_s}\right) + \frac{1}{3}\left(\frac{T_{0_t}}{T_s}\right)^4 \right) \quad (14)$$

For conductive heat transfer, exergy is estimated according to Eq. 15:

$$E_{int_{layer_{i,t} \to layer_{i+1,t}}} = Q_{int_{layer_{i,t} \to layer_{i+1,t}}} \left(1 - \frac{T_{0_t}}{T_{i,t} - T_{i+1,t}} \right) \quad (15)$$

Eq. 15 specifies the conductive heat transfer for the NCZ region, which is divided into individual sub-layers, and hence the interface temperature is used, whereas for the LCZ and UCZ the average temperature is used [16].

The exergy of the extracted energy may be determined using the same exergy equation as in the exergy stored. However, in this case, similar to energy analysis, instead of using the mass, mass flow rate $\dot{m}_{ext_t}$ (kg/s) and extractions time *Time (s)* is used (Eq. 16). The dead state assumed in exergy analysis is T_0 = 250 °C and P_0 =101kPa.

$$E_{ext_t} = \dot{m}_{ext_t} \cdot Cp \cdot \left(\left(T_{ext_t} - T_{in_t} \right) - \left(T_0 \ln \left(\frac{T_{ext_t}}{T_{in_t}} \right) \right) \right) * Time \quad (16)$$

Part of the system's exergy is lost to the environment and another part is destroyed due to irreversibility. In energy analysis, the variable $Q_{loss_{layer_i}}$ contains different types of energy losses, but determining the exergy associated with this parameter is not possible. In that context, exergy losses and exergy destroyed are considered in the same variable as useless exergy. The methodology for calculating exergy destroyed as equal to useless energy as described in Eq. 17 is based on similar exergy studies on solar pond technology [16].

$$\begin{aligned} E_{useless_i} = \sum_0^t \Big[& E_{S_{abs}\,layer_{i,t}} + E_{int_{layer_{i+1} \to layer_{i,t}}} \\ & + E_{int_{layer_{i-1,t} \to layer_{i,t}}} \Big] \\ & - \sum_0^t \Big[E_{int_{layer_{i,t} \to layer_{i+1,t}}} + E_{int_{layer_{i,t} \to layer_{i-1,t}}} \\ & + E_{stored_{layer_{i,t}}} \left(+ E_{ext_t} \right) \Big] \end{aligned} \quad (17)$$

2.4 Energy and exergy efficiencies

Different models to determine the efficiency of solar ponds are defined in the literature [7, 15, 16, 35-37]. Both energy and exergy efficiencies are defined as the ratio between the useful energy/exergy and the total input energy/exergy to the system. In a solar pond system, useful energy/exergy correspond to the stored and extracted fluxes, and the input energy/exergy are associated with the solar radiation. However, estimating the efficiency of each zone is important to understand the function of each layer and how it

affects the overall operation of the solar pond technology. In this case, the input energy/exergy also contains internal gains.

An instantaneous efficiency analysis can be considered as suggested by Date et al. [33]; however, it has important shortcomings. First, the instantaneous efficiency in periods when the solar pond is storing energy is not representative of the global efficiency of the system. Second, the heat extracted in a given period is not a result of the instantaneous solar radiation but rather the result of previously stored solar radiation. Third, in periods when the solar pond is not storing energy/exergy and when no heat extractions take place, an efficiency of 0% would be obtained, which is not representative.

These shortcomings may be overcome by considering longer periods. Alcaraz et al. [3] suggested that the overall efficiency of the system could be determined as the average of all monthly efficiencies.

As previously said, the heat stored at a given period of time may be used some months later. For that reason, a cumulative model is suggested in this work. Hence, the energy and exergy efficiencies at the end of a period consider all events that have occurred since the beginning of the operation period. Thus, the energy and exergy efficiencies of each layer are determined through Eq. 18 and 19, respectively:

$$\eta = \frac{\sum_0^t \left[Q_{stored_{layer_{i,t}}} + Q_{ext_t} \right]}{\sum_0^t \left[Q_{S_{abs\,layer_{i,t}}} + Q_{int\,layer_{i+1,t} \rightarrow layer_{i.t}} + Q_{int\,layer_{i-1,t} \rightarrow layer_{i,t}} \right]} \quad (18)$$

$$\psi = \frac{\sum_0^t \left[E_{stored_{layer_{i,t}}} + E_{ext_t} \right]}{\sum_0^t \left[E_{S_{abs\,layer_{i,t}}} + E_{int\,layer_{i+1} \rightarrow layer_{i,t}} + E_{int\,layer_{i-1,t} \rightarrow layer_{i,t}} \right]} \quad (19)$$

The overall efficiencies of a solar pond are determined considering all the layers of the system. Additionally, when the whole system is analysed the internal heat transfers are compensated. Eq. 20 and 21 are used to determine the overall energy and exergy efficiency of the system:

$$\eta = \frac{\sum_0^{i=L_{TOT}} \sum_0^t \left[Q_{stored_{layer_{i,t}}} + Q_{ext_t} \right]}{\sum_0^{i=L_{TOT}} \sum_0^t \left[Q_{S_{abs\,layer_{i,t}}} \right]} \quad (20)$$

$$\psi = \frac{\sum_0^{i=L_{TOT}} \sum_0^t \left[E_{stored_{layer_{i,t}}} + E_{ext_t} \right]}{\sum_0^{i=L_{TOT}} \sum_0^t \left[E_{S_{abs\,layer_{i,t}}} \right]} \quad (21)$$

2.5 Thermoeconomic analysis

Thermoeconomics is an important branch of engineering that combines the theories and methodologies of thermodynamics and economics [38]. The exergy associated with the different variables that intervene in the system are taken as the basis for the allocation of economic costs between the different input and output flows. Mathematically, a thermoeconomic analysis may be described by Eq. 22 as proposed by Oliviera et al. [39]:

$$\sum_k \dot{\Pi}_{ik} + \dot{Z} = \sum_l \dot{\Pi}_{ol} \quad (22)$$

where $\dot{\Pi}_{ik}$ is the economic value of the input exergy fluxes to the system, $\dot{Z}$ is the total capital costs including the investment and operation and maintenance costs, and $\dot{\Pi}_{ol}$ is the economic value of the output exergy fluxes from the system. In turn, $\dot{\Pi}$ may be calculated through Eq. 23:

$$\dot{\Pi} = c \cdot \dot{E} \quad (23)$$

where c is the price associated with the exergy flux and $\dot{E}$ is the corresponding exergy flux.

The solar pond is a complex system because part of the input flux is stored in the system for a long period of time. Hence, there is no balance between the input and output fluxes. In the literature, none of the existing solar ponds, industrial or pilot plants have been analysed from the thermoeconomic point of view. In that context, an exhaustive literature review was carried out to identify thermoeconomic analyses that have been applied in different technologies and that may be useful to develop a methodology to analyse a solar pond technology. The methodology developed by Kazim et al. [40] to thermoeconomically evaluate a fuel cell may have a certain parallelism with the solar pond.

First, the fuel cell was analysed as a black box, i.e., the system was studied as a whole and the different elements were not independently analysed. The solar pond analysis follows the same principle and it is analysed as a whole. However, the fuel cell charge–discharge cycles were relatively short. Hence, the authors considered hydrogen and air as inputs, and water, air and electricity as outputs. The analysis omitted the time variable for the energy stored in the fuel cell.

In a solar pond, part of the heat stored in the system will not be extracted. Once the system starts its operation, the temperature inside the LCZ will never return to its initial value. Despite part of the heat stored never being used, this part of the heat has an economic value for the owner of the facility because it is an important reserve that may be used in case of necessity.

In that context, the model suggested to analyse a solar pond from the thermoeconomic point of view can be determined using Eq. 24:

$$c_{solar}\dot{E}_s + \dot{Z}_{SP} = c_{ext}\dot{E}_{ext} + c_{stored}\dot{E}_{stored} \quad (24)$$

where c_{solar} is the exergy cost of the solar exergy ($\dot{E}_s$), c_{ext} is the exergy cost of the exergy extracted from the system ($\dot{E}_{ext}$), c_{stored} is the exergy cost of the exergy stored in the system ($\dot{E}_{stored}$) and $\dot{Z}_{SP}$ is the annual cost of the system, which includes a proportional part of the investment cost and the operation and maintenance costs, which can be determined according to Eq. 25:

$$\dot{Z}_{SP} = \dot{Z}_{CI} + \dot{Z}_{OM} \quad (25)$$

where $\dot{Z}_{CI}$ is the annual investment cost and $\dot{Z}_{OM}$ the annual operation and maintenance cost. Although the investment cost is paid during the construction of the solar pond, the annual capital cost is considered. The annual capital cost considers both the investment cost and economic inflation. Thus, the annual capital cost may be determined through Eq. 26:

$$Z_{CI} = Inv.Cost \cdot \frac{i_r(1+i_r)^{n_y}}{(1+i_r)^{n_y}-1} \quad (26)$$

where $Inv.Cost$ is the investment cost, i_r is the inflation rate and n_y is the lifetime of the system. The annual operation and maintenance cost, $\dot{Z}_{OM}$, is determined as a percentage of the investment cost.

3. Results and discussion

3.1. Energy and exergy efficiencies

The solar pond in Granada started its operation in July 2014. The density in the LCZ was kept almost constant for 10 months with an average value of 1203 kg/m^3 and the temperature evolved according to the weather conditions. The initial temperature in the LCZ recorded in the solar pond once the salinity gradient was established was 42.7 °C. Thanks to the high solar radiation during the first month, the temperature in the LCZ increased by 1.5 °C per day on average, reaching a maximum temperature of 89 °C at the end of August 2014 as can be seen in Figure 2. The degradation of the salinity gradient was detected by the density profile monitoring as the height to the UCZ increases from 0.3 m in July 2014 to 0.8 m in April 2014. Although the same trend was observed in the evolution of the temperature profile, the average monthly temperature of the LCZ not decreased below 40 °C (Figure 2). After a second refilling process in 2016, the Granada solar pond operated successfully until March 2020, when the mine facility restricted its operation due to the pandemic situation.

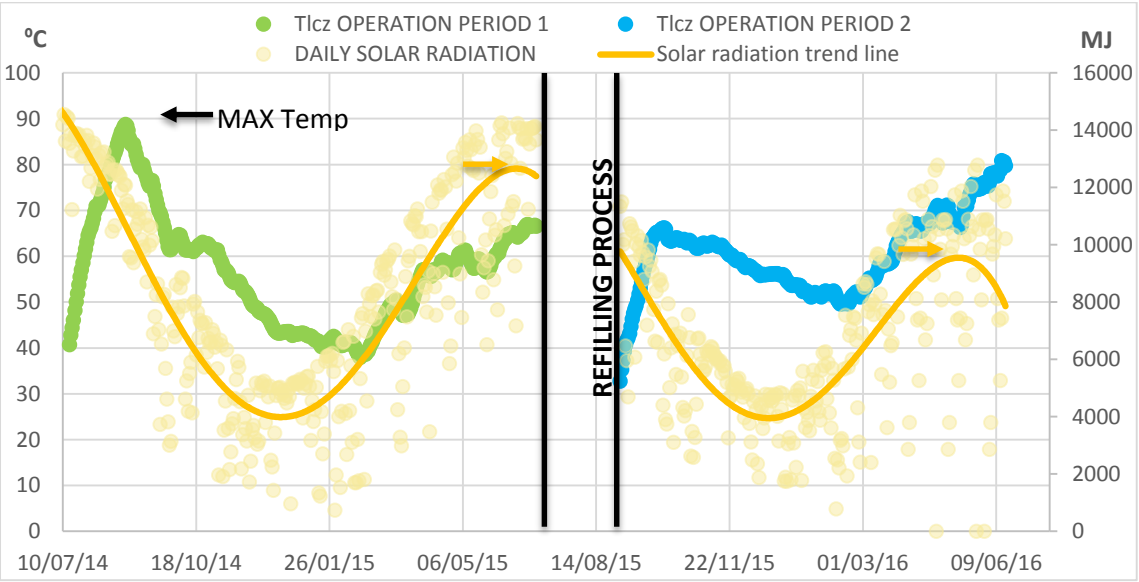

Figure 2. Evolution of the LCZ average temperature along the first and second operation periods of the Granada solar pond.

The Granada solar pond is evaluated from the energy point of view. Figure 3 represents the energy analysis of the three zones of the system. As can be seen in Figure 3a, the UCZ cannot store energy; almost all the solar radiation absorbed by this zone is lost through the surface, evaporative and convective losses, and the walls. The efficiency of this zone is not analysed because there is no storage or heat extraction.

The NCZ (Figure 3b) has a small capacity to store part of the solar radiation, especially in the first months. The main aim of the NCZ is to prevent heat stored in the LCZ from escaping, i.e. it works as an insulator. Thus, the isolation of the lowest sublayers of the NCZ results in a notable capacity of the system to store heat. The low temperature of the water during the filling and the high ambient temperature and solar radiation in summer resulted in an increase in the energy stored in the NCZ. However, in winter, the system was not capable of retaining the heat stored in the NCZ. The system started to store again in the NCZ when the environmental conditions were notably better. The energy stored in the zone has a direct impact on the energetic efficiency. The NCZ reported an efficiency of almost 60% in the first month of operation that decreased to 0% in the winter months because of the heat losses. As this work considered a cumulative analysis of the system, the efficiency obtained at the end of the operation period is the overall efficiency of the zone. This efficiency considers all the environmental events that occurred since the operation started. Thus, the NCZ has an overall efficiency of 3.4% and 5.9% in the first and second operation periods, respectively.

The large capacity and potential of the system to store heat is clearly represented in Figure 3c, which contains the analysis of the LCZ. The LCZ is the zone in the solar pond that provides heat to an external application, in this case the flotation stage at Solvay Minerales facilities. In the first operation period, the fraction of stored energy increased abruptly in the first months of operation, due to the good environmental conditions and due to the large capacity of the system, thereby increasing its temperature.

In September, the system started to lose part of the energy stored. However, the LCZ always kept a significant amount of stored heat, even under adverse environmental conditions. In March 2014, due to the improvement in environmental conditions the LCZ started to increase the stored energy, thereby increasing its temperature. Throughout the year, even in the winter months, a significant amount of energy was extracted from the system. As a result, the LCZ, when independently analysed, shows high efficiency. The large capacity of the system to store energy at the beginning of the operation period resulted in efficiencies of 57.8% and 46.6% after the first and second month of operation, respectively. The lowest energy efficiency registered in the LCZ was 19.6%, when the first six months of operation were considered. After one year of operation, the overall efficiency of this zone was 23.1%.

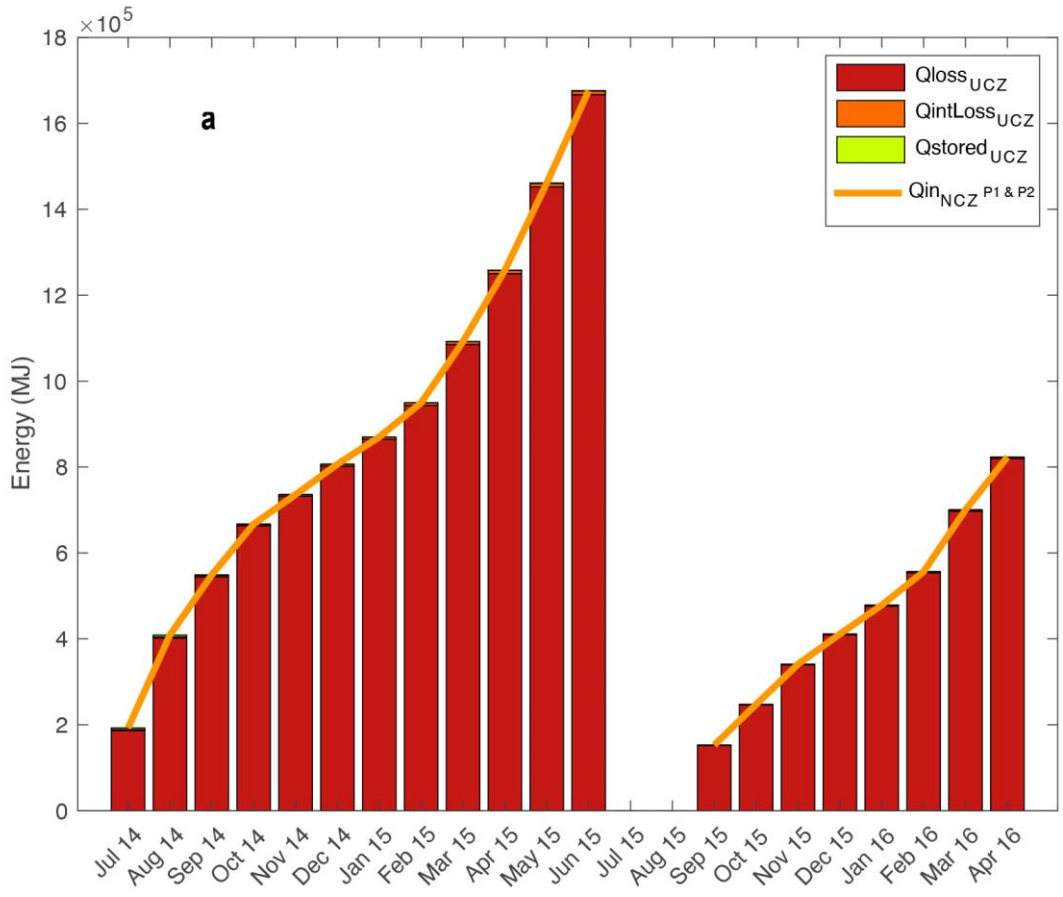

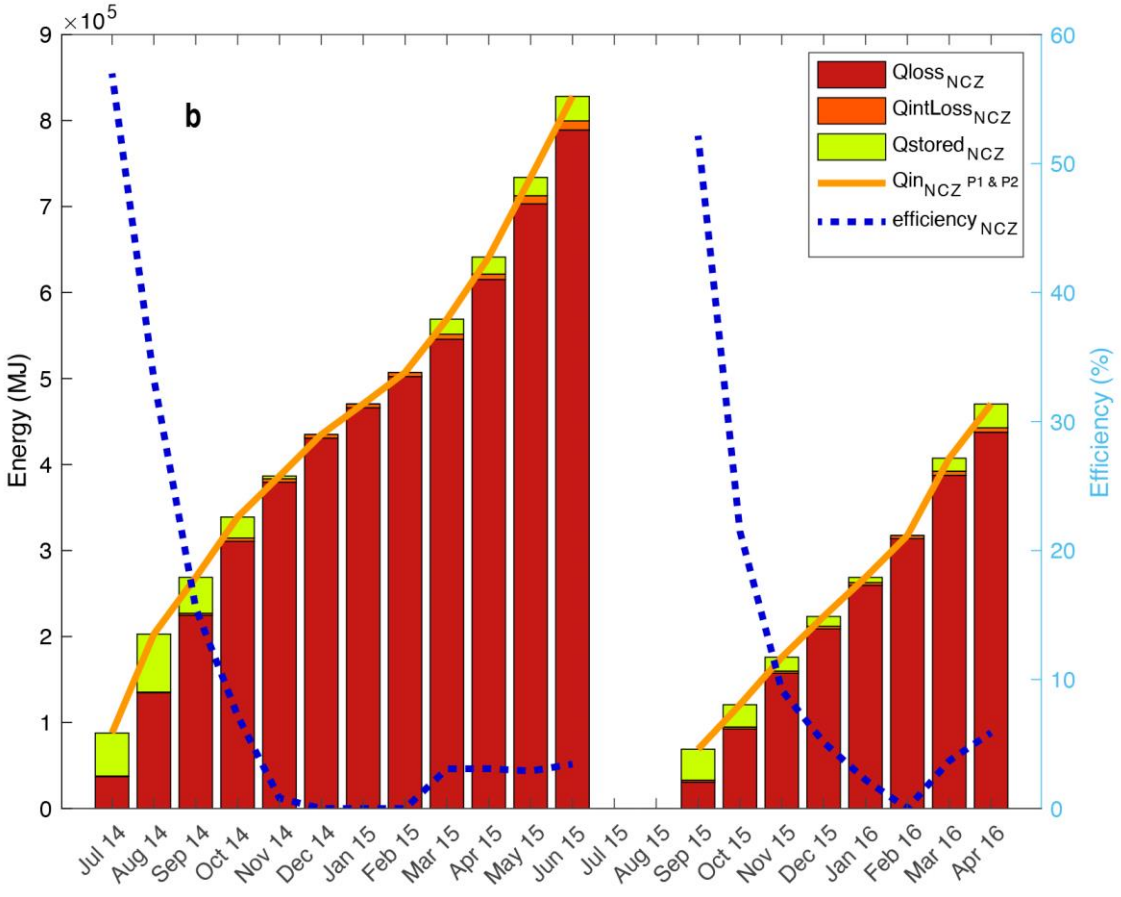
×10^5
b
Qloss NCZ
QintLoss NCZ
Qstored NCZ
Qin NCZ P1 & P2
efficiency NCZ
Energy (MJ)
Efficiency (%)
0
1
2
3
4
5
6
7
8
9
0
10
20
30
40
50
60
Jul 14
Aug 14
Sep 14
Oct 14
Nov 14
Dec 14
Jan 15
Feb 15
Mar 15
Apr 15
May 15
Jun 15
Jul 15
Aug 15
Sep 15
Oct 15
Nov 15
Dec 15
Jan 16
Feb 16
Mar 16
Apr 16

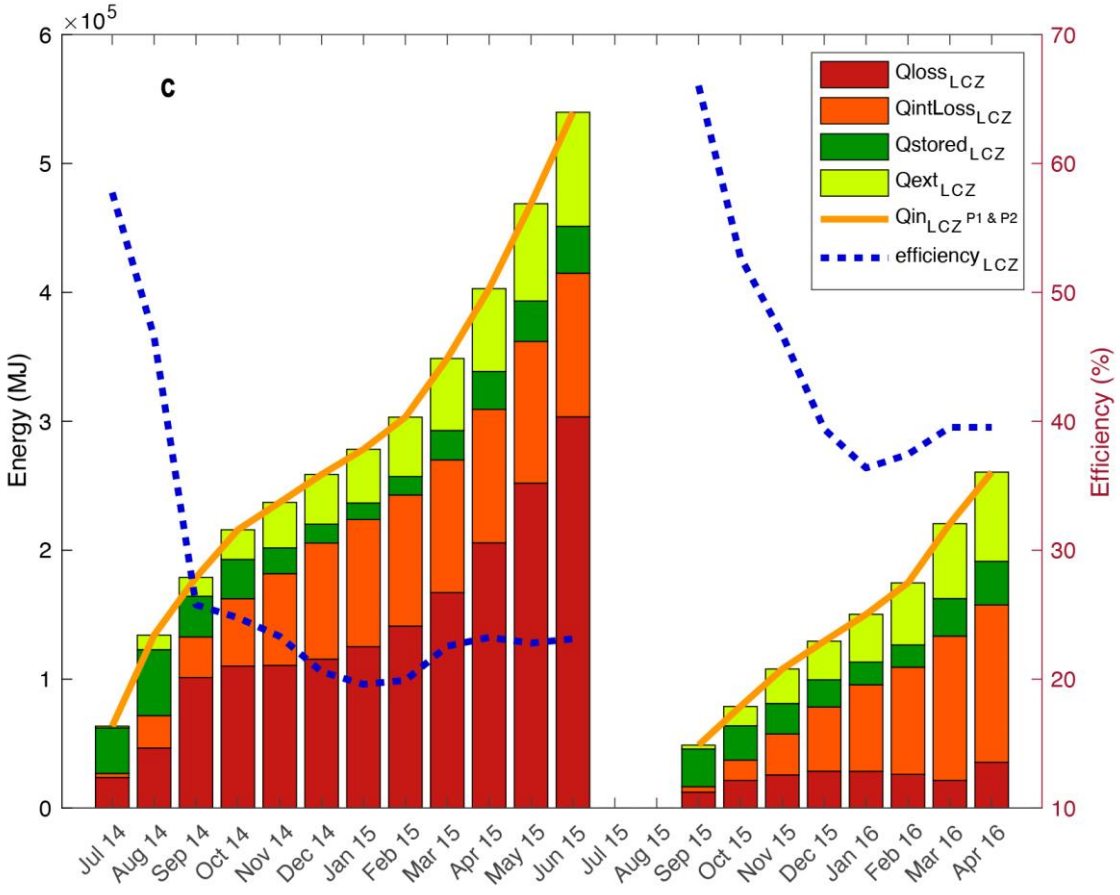

Figure 3. Energy fluxes and efficiency of: a) UCZ, b) NCZ and c) LZC during the first and second operation periods of the Granada solar pond (blue line indicates efficiency).

In the second operation period, despite starting the operation in September 2015, the system was able to increase the stored energy and provide heat to the flotation stage. The amount of heat stored in the pond started to decrease from November 2015 to February 2016, when the stored heat increased again. In the second period of operation, a greater amount of heat was extracted from the system. Heat extraction has a positive impact on the system because it increases the capacity of the solar pond to store energy. As a result, higher efficiencies were achieved in the second operation period. The efficiency after the first and second months of operation was 66.0% and 52.7%, respectively. The lowest efficiency in this operation period was 36.4% registered in January 2016. The overall efficiency at the end of the second operation period was 39.6%.

Considering the energy analysis, the UCZ and the NCZ are essential in the system to ensure the proper operation of the solar pond. In this sense, maximizing heat extraction will increase the energy and exergetic efficiency of the solar pond by increasing the storage capacity; this can be achieved by optimizing the operation of the flotation unit that allows increasing the mineral treatment during the months of high radiation. However, the LCZ is the part of the system that produced an energetic value due to its capacity to store and provide heat. Thus, the exergy analysis is focused on the LCZ and is compared with the energy analysis.

All the energy and exergy fluxes of the LCZ are shown in Figure 4. Exergy analysis is less favourable than energy analysis because not all energy is always useful. The greater the difference between the temperature of the energy flux and the ambient air temperature, the greater the exergy, i.e., the more useful is the energy flux. The internal heat transfers and the heat stored decreased notably due to the small difference between the LCZ temperature and the ambient air temperature. The maximum and minimum monthly mean differences were 55.5ºC in August 2014 and 29.8ºC in January 2015, respectively, during the first operation period, and 55.9ºC in April 2016 and 33.0ºC in September 2015, respectively, during the second operation period. The efficiency of the heat exchanger installed at the bottom of the pond resulted in a lower temperature of the water inside the heat exchanger than the LCZ temperature. As a consequence, the heat extraction is the variable with the smallest difference between its temperature range and the ambient temperature. Hence, the exergy of the heat extracted is much lower than the energy of this heat flux.

The heat stored and heat extracted were much lower in percentage than the solar radiation in the exergy analysis. As a consequence, the values obtained for the exergy efficiency are clearly much lower than for the energy analysis as has been reported in previous studies [15-20]. The overall exergy efficiency of the LCZ after the first and second operation periods was 1.6% and 2.3%, respectively.

As in the energy analysis, increasing the amount of heat extracted from the system improves the exergy efficiency. As a result, the exergy efficiency was significantly higher in the second operation period.

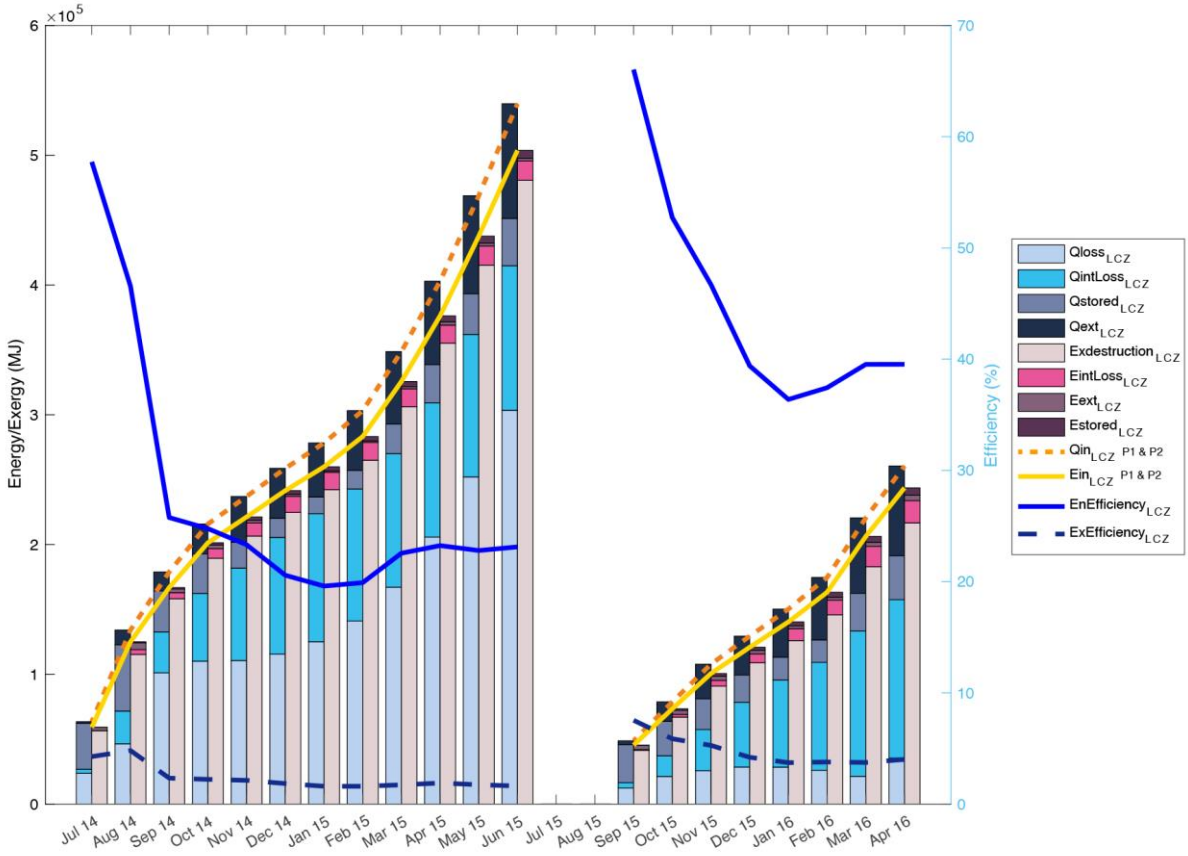

Figure 4. Energy and exergy fluxes and efficiencies of the LCZ during the first and second operation periods of the Granada solar pond.

Finally, the overall energy and exergy performance of the Granada solar pond is compared in Figure 5. As for the energy analysis, the energy efficiency is less favourable when the whole system is considered than when the LCZ is independently analysed as a consequence of the whole system being influenced by the low efficiencies of the NCZ and the UCZ. As has been said, the NCZ and the UCZ have low efficiencies because these zones have a low capacity to store heat and no heat extractions are carried out. However, thanks to the UCZ and the NCZ, the LCZ has a large capacity to store heat and consequently a large efficiency. At the end of the first operation period the overall efficiency of the system

was 5.3%, and 9.0% at the end of the second operation period. Once again, the larger amount of heat extracted from the system is reflected in the higher overall efficiency of the system.

The results of the exergy follow the same trend; the exergy efficiency of the whole system is clearly lower than the exergy efficiency of the LCZ due to the influence of the NCZ and UCZ. Additionally, the exergy efficiency is always lower than the energy efficiency since exergy only considers the fractions of energy that may be useful. This fraction is higher with a larger difference between the temperature of the energy flux and the ambient air temperature. The Granada solar pond registered a maximum temperature in the LCZ of almost 92ºC during the operation period 2014–2015 [3]. Therefore, the solar pond works at temperatures close to room temperature and consequently the exergetic efficiency decreases significantly. The overall exergy efficiency at the end of the first and second operation period of the solar pond was 0.34% and 0.43%, respectively. Those values are in agreement with those reported for small solar ponds or in modelling analyses [10-16].

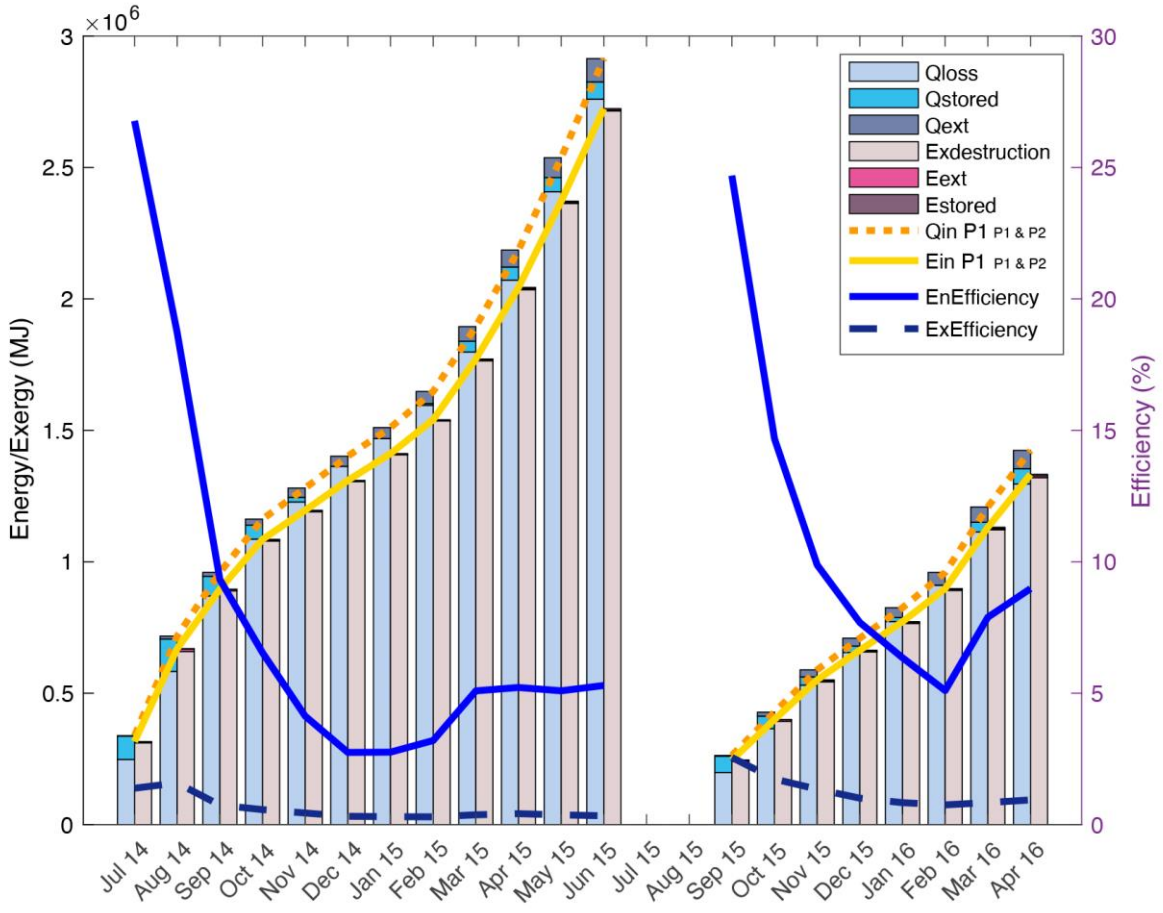

Figure 5. Overall energy and exergy fluxes and efficiencies during the first and second operation periods of the Granada solar pond.

3.2. Thermoeconomic analysis

In this section, the results of the thermoeconomic analysis are reported. The assumptions and input data are initially described followed by the detailed results. As defined in section 2.5. (Thermoeconomic analysis), apart from the exergy, the costs associated with each exergy flux are necessary to analyse a solar pond from the thermoeconomic point of view.

The cost associated with the input exergy, the solar exergy (c_{solar}), can be assumed in 0 €/MJ. The sun is always available and it is completely free for the owners of the facility. The input exergy of the solar pond being completely free is an important advantage for the technology. The main aim of the solar pond built in Granada is to reduce the amount of fuel oil used to heat the water needed at the flotation stage.

Fuel oil, apart from being a fossil fuel that pollutes in being used, is also expensive. The cost associated with the extracted exergy (c_{ext}) is more difficult to quantify. As the extracted exergy directly means a reduction in the fuel oil consumed, the value attributed to the extracted exergy flux is the fuel oil cost.

Different scenarios are found in the literature regarding the evolution of fuel oil prices. In this work, the approximation of fuel oil prices reported by EIA [41] is considered. In this scenario, the fuel oil prices are expected to increase from 0.025 $/MJ in 2020 to 0.0325 $/MJ by 2050. The evolution of the fuel oil prices has been detailed in section 2 of the Supplementary Material.

To determine the annual capital cost ($\dot{Z}_{SP}$), which is composed of the investment and operation and maintenance costs, the values reported in Valderrama et al. [42] are considered. The investment cost of the Granada solar pond was approximately 190 $/m^2, out of which 67 $/m^2 were fixed costs that are independent of the surface of the installation and 123 $/m^2 were variable and depended on the surface of the solar pond. The annual investment cost depends on the inflation rate of the economy and the lifetime of the facility. The economic inflation is initially assumed as 3% and the lifetime of the facility is approximately 30 years. As for the annual operation and maintenance cost, a percentage of 3% of the total investment cost was assumed, as reported in Valderrama et al. [42].

As previously introduced, the exergy stored in the system may have an important value because it is an important reserve that could be used in case of necessity. This cost (c_{stored}) is uncertain since it is difficult to be estimate and no references were found in the literature. Therefore, the cost of exergy stored is assessed in this work. In that context, two different thermoeconomic analyses are suggested. In the first analysis, c_{stored} is considered as the unknown variable. Hence, considering 3% inflation and the actual dimensions of the solar pond, the minimum cost associated with the exergy stored, which ensures the thermoeconomic feasibility of the solar pond, is determined. In the second analysis, the exergy stored is considered as a fuel oil reserve. Hence, the price of fuel oil is attributed to this exergy flux. In this

second approach, the minimum surface that ensures the thermoeconomic feasibility of the solar pond under different scenarios of inflation and investment cost reduction was determined.

Apart from the cost, the exergy results reported in section 3.1 are considered. In Figure 6, the exergy stored in the system and the exergy extracted from it during the first and second operation periods are independently plotted. Similar results are obtained in both operation periods. Regarding the exergy stored, the different time intervals during the first and second periods and the nature of the months during their respective operations may lead to small differences as can be seen in Figure 6a. The exergy extracted from the system is more difficult to predict due to the fact that heat is extracted according to the energy demand of the flotation stage leading to a higher level of uncertainty.

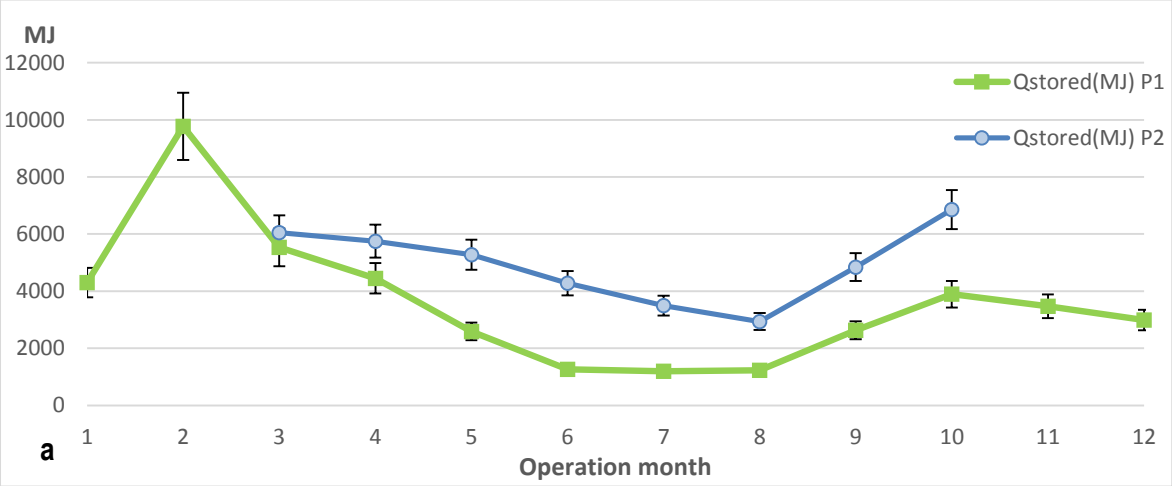

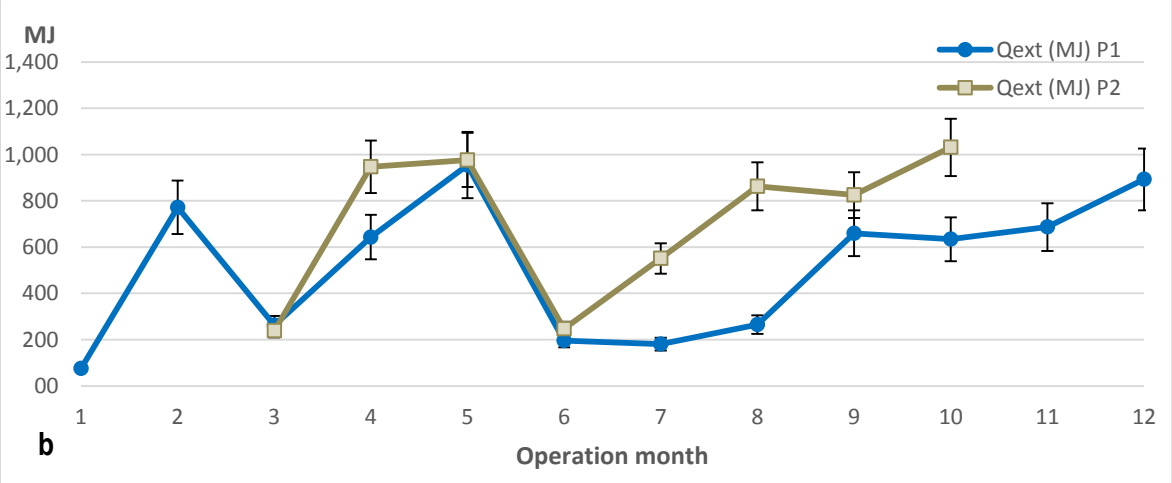

Figure 6. a) Exergy stored during the first and second operation period, and b) exergy extracted from the system during the first and second operation period in the Granada solar pond.

In that context, and as an approximation, the average values of both the stored and extracted exergies are considered in this analysis. Additionally, both variables are considered constant over time as a better approximation of the stored and extracted exergy is not possible. This is because the solar radiation tends to be constant over time and the exergy extracted cannot be predicted because of the irregular and unpredictable external demands.

3.3 Minimum price for the exergy stored

In this section, the actual dimensions of the solar pond are considered to determine the minimum cost associated with the exergy stored that ensures the thermoeconomic feasibility of the system. As previously introduced, the annual exergy extracted from the system and the annual exergy stored in the system are considered constant over the lifetime, i.e., every year the same amount of exergy is extracted from the system and stored. Regarding the annual capital cost, when 3% economic inflation and a 30-year lifetime are considered, the annual capital cost rises to 7696.8 $/year, where 4846.8 $/year can be referred to the annual investment cost and 2850 $/year to the operation and maintenance cost. The annual capital costs are constant over the lifetime. Additionally, as 0 $/MJ is assumed for solar exergy, this parameter can be neglected in the analysis. Thus, all the variables considered in the analysis are constant over the lifetime of the solar pond except the fuel oil cost, which tends to increase with time. The increase in fuel oil prices is an important advantage for the solar pond's feasibility as higher costs of fuel oil prices result in higher savings from solar pond utilisation.

The price evolution of the heat stored in the pond is determined according to Eq. 24, described in section 2.5, which makes the facility feasible from the thermoeconomic point of view. Figure 6 shows the necessary evolution in the price of exergy stored. As expected, the cost tends to decrease inversely to the fuel oil price. The increase in fuel oil prices improves the thermoeconomic feasibility of the facility, thereby reducing the cost of exergy stored.

Comparing the minimum annual cost necessary in the exergy stored in the system (Figure 7) with the fuel oil prices evolution, the cost of the exergy stored needs to be between 4 and 5 times higher than the fuel oil price. Although the exergy stored in the system has a monetary value, this price will hardly be higher than the fuel oil price. Thus, it can be concluded that the current facility cannot be considered feasible from the thermoeconomic point of view. At the current level of development, the technology would only be feasible if economic incentives such as taxes or subsidies were to be received.

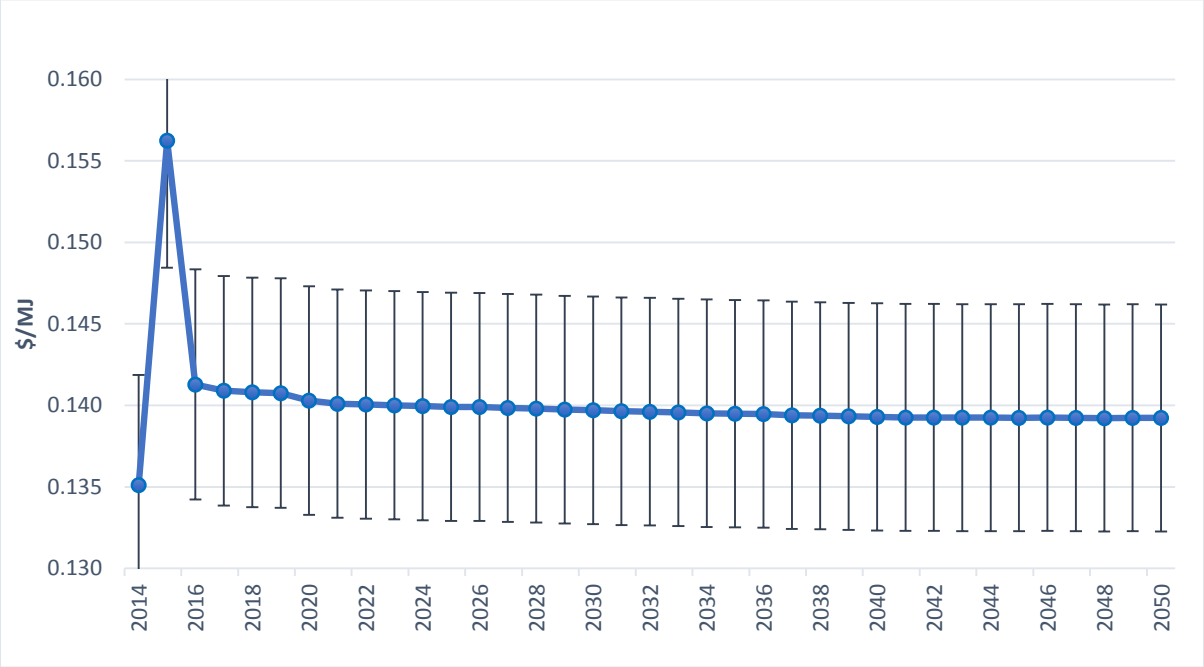

Figure 7. Minimum annual cost of exergy stored in the Granada solar pond to ensure the thermoeconomic feasibility.

3.4 Minimum surface to ensure the thermoeconomic feasibility under different scenarios

According to Valderrama et al. [42], technologies such as solar ponds take advantage of economies of scale and it would therefore be expected that larger surfaces will have better thermoeconomic results. In this study, as previously described, the exergy stored in the solar pond is assumed as a fuel oil reservoir and the fuel oil prices are consequently associated with it. The difficulty is in quantifying the amount of energy stored and extracted from the system. The exergy extracted from the system depends on external needs and it is not constant. In that context, and as an approximation, the exergy stored and extracted

under different surfaces is calculated proportional to the exergy stored and extracted under the current solar pond (500 m^2). The minimum surface area needed to make the solar pond technology feasible is determined under different scenarios involving cost reduction and economic inflation as shown in Figure 8. The analysis evaluates 5 different inflation rates (1%, 2%, 3%, 4% and 5%) and under a range of cost reductions between 51 and 80%. A minimum cost reduction of 51% is considered because below this percentage the technology is not feasible under any inflation rate.

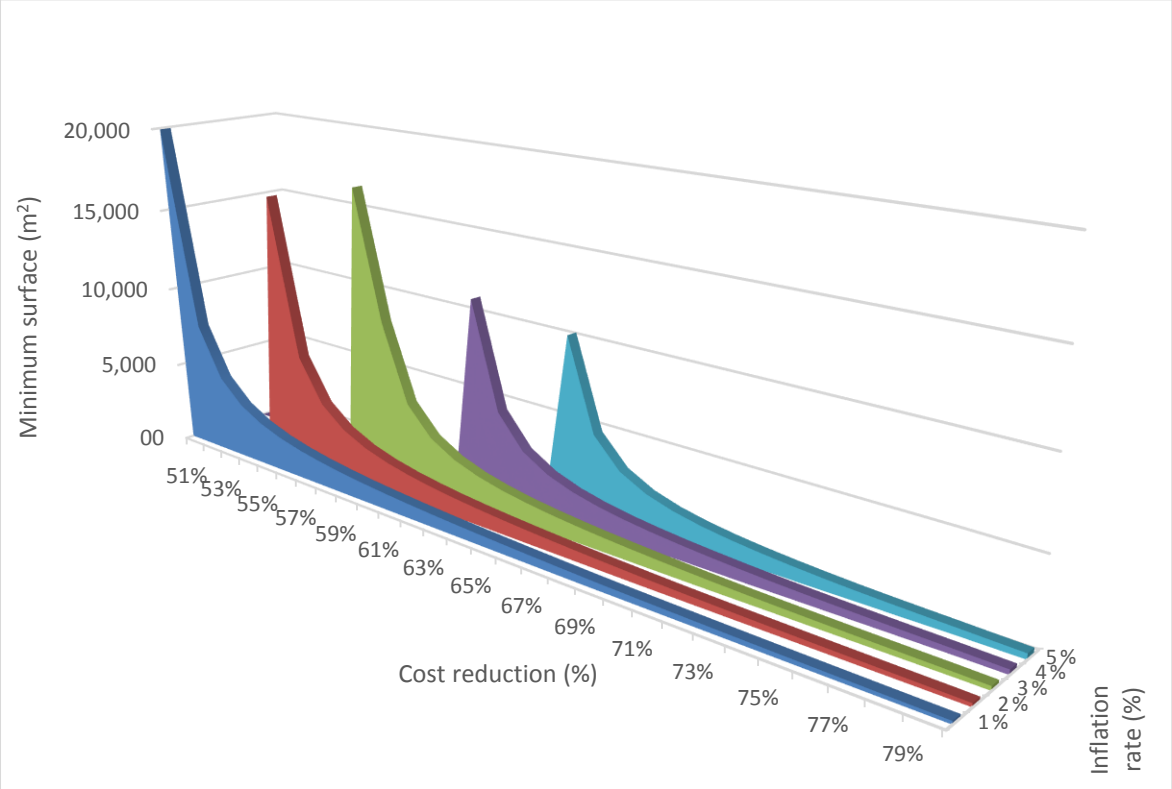

Figure 8. Minimum surface to ensure the thermoeconomic feasibility of the Granada solar pond under different inflation and cost reduction rates.

As shown in Figure 8, by setting the inflation rate, the surface can be reduced by increasing cost reductions. For a fixed percentage of cost reduction, the solar pond can be a feasible technology with a minimal footprint by lowering the inflation rate. In addition, at higher inflation rates, higher cost reduction rates are needed to make the solar pond feasible; that is, with inflation below 2%, a minimum cost

reduction of 55% is necessary. The larger the solar pond, the higher the inflation rates and lower the cost reduction rates that can be accommodated, as has also been reported by Valderrama et al. [42].

It is worth mentioning that this analysis is carried out assuming that the energy stored as a fuel oil deposit and this may lead to an unrealistic interpretation of the behavior of the solar pond from a thermoeconomic point of view. The objective was to consider evaluating the exergy cost of the energy stored in the solar pond, which is variable over time, to determine the thermoeconomic viability of the Granada solar pond, estimating either the minimum cost of stored exergy or the minimum area to ensure such feasibility. The results indicate that this depends largely on the fluctuation of the replaced fossil fuel market, the amount of heat extracted, which is also variable, and the capacity of the solar pond to store exergy in the LCZ, highly dependent on the heat extracted, environmental conditions, and its maintenance and operation. This first attempt to estimate the thermoeconomic viability of an industrial solar pond reveals that it is more complex than other energy storage systems described in the literature due to the variability of some of the processes involved. Future work should therefore consider new approaches to reduce uncertainty in the modeling of the system.

4. Conclusions

The overall energy efficiencies of the Granada solar pond were 5.79% and 8.98% after the first and second operation period, respectively. The exergy analysis reported overall efficiencies of 0.34% and 0.43%, respectively. This significant difference between the energy and exergy analysis is due to the fact that the exergy considers the useful part of the energy flux. It is also observed that heat extraction plays an important role in the efficiency of the solar pond, by increasing the amount of heat extracted, it also increases the storage capacity and consequently the energy and exergetic efficiency of the system increases. The thermoeconomic analysis of the Granada solar pond indicated that this installation is not feasible with the current investment, maintenance costs, and considering the amount of fossil fuel savings. Estimating the cost of the stored exergy is the main source of uncertainty due to the variability of the processes involved and it can lead to erroneous interpretations when evaluating the viability of a

solar pond from a thermoeconomic perspective. According to assumption considered in the current study, to be feasible, the cost of the exergy stored in the system must be between 4 and 5 times higher than the cost of fuel oil, in addition to providing economic incentives or tax reductions. In addition, the minimum surface area required to make the system feasible under different scenarios was estimated (between 10000 and 20000 m^2). Future research will focus on improving the efficiency of solar pond technology by increasing storage capacity (increasing and optimizing heat extraction based on energy demand), on the other hand, the thermoeconomic performance of solar pond will depend of the variability of the price of fossil fuels and economies of scale, as has been shown in this study.

Acknowledgments

We would like to gratitude the Spanish Ministry of Economy and Competitiveness (MINECO) for the Waste2Product project (CTM2014-57302-R), the R2MIT project (CTM2017-85346-R) and the Catalan Government (2017-SGR-312). Finally, the authors gratefully acknowledge personnel from Solvay Minerales and Solvay Martorell facilities for practical assistance, especially to M. Gonzalez, C. Gonzalez, C. Aladjem, and M. Giménez for their valuable cooperation.

5. References

1. Tabor, H.Z. and B. Doron, *The Beith Ha'Arava 5 MW(e) Solar Pond Power Plant (SPPP)—Progress report.* Solar Energy, 1990. **45**(4): p. 247-253.
2. Tabor, H. and B. Doron, *Solar Ponds-Lessons learned from the 150 kW (e) power plant at Ein Boqek.* Proc. of the ASME Solar Energy Div., Anaheim, California, 1986.
3. Alcaraz, A., et al., *Design, construction, and operation of the first industrial salinity-gradient solar pond in Europe: An efficiency analysis perspective.* Solar Energy, 2018. **164**: p. 316-326.
4. Cao, Y., et al., *Thermo-economic evaluation of a combined Kalina cycle and humidification-dehumidification (HDH) desalination system integrated with thermoelectric generator and solar pond.* International Journal of Heat and Mass Transfer, 2021. **168**: p. 120844.
5. Kalogirou, S.A., *Solar energy engineering: processes and systems*. 2013: Academic Press.
6. Dincer, I. and M. Rosen, *Thermal Energy Storage (TES).* Thermal Energy Storage: Systems and Applications, 2002: p. 93.
7. Leblanc, J., Akbarzadeh, A., Andrews, J., Lu, H., Golding, P., 2011. Heat extraction methods from salinity-gradient solar ponds and introduction of a novel system of heat extraction for improved efficiency. Sol. Energy. doi:10.1016/j.solener.2010.06.005

8. Verma, S., Das, R. Transient study of a solar pond under heat extraction from non-convective and lower convective zones considering finite effectiveness of exchangers. Sol. Energy 2021. 223, 437–448.
9. Verma, S., Das, R. Effect of ground heat extraction on stability and thermal performance of solar ponds considering imperfect heat transfer. Sol. Energy 2020. 198, 596-604. doi.org/10.1016/j.solener.2020.01.085
10. Khalilian, M., H. Pourmokhtar, and A. Roshan, *Effect of heat extraction mode on the overall energy and exergy efficiencies of the solar ponds: A transient study.* Energy, 2018. **154**: p. 27-37.
11. Verma, S., Das, R. Revisiting Gradient Layer Heat Extraction in Solar Ponds Through a Realistic Approach. J. Sol. Energy Eng. 2020. 142(4): 041009. doi.org/10.1115/1.4046149
12. Ranjan, K., S. Kaushik, and N. Panwar, *Energy and exergy analyses of solar ponds in the Indian climatic conditions.* International Journal of Exergy, 2014. **15**(2): p. 121-151.
13. El Mansouri, A., et al., *Transient theoretical model for the assessment of three heat exchanger designs in a large-scale salt gradient solar pond: Energy and exergy analysis.* Energy Conversion and Management, 2018. **167**: p. 45-62.
14. Njoku, H.O., B.E. Agashi, and S.O. Onyegegbu, *A numerical study to predict the energy and exergy performances of a salinity gradient solar pond with thermal extraction.* Solar Energy, 2017. **157**: p. 744-761.
15. Bozkurt, I. and M. Karakilcik, *Exergy analysis of a solar pond integrated with solar collector.* Solar Energy, 2015. **112**: p. 282-289.
16. Dehghan, A.A., A. Movahedi, and M. Mazidi, *Experimental investigation of energy and exergy performance of square and circular solar ponds.* Solar energy, 2013. **97**: p. 273-284.
17. Khalilian, M., *Exergetic performance analysis of a salinity gradient solar pond.* Solar Energy, 2017. **157**: p. 895-904.
18. Khalilian, M., *Assessment of the overall energy and exergy efficiencies of the salinity gradient solar pond with shading effect.* Solar Energy, 2017. **158**: p. 311-320.
19. Njoku, H.O., Agashi, B.E., Onyegegbu, S.O., A numerical study to predict the energy and exergy performances of a salinity gradient solar pond with thermal extraction. Solar Energy 2017. 157: p. 744-761.
20. Khalilian, M., Pourmokhtar, H., Roshan, A., Effect of heat extraction mode on the overall energy and exergy efficiencies of the solar ponds: A transient study. Energy, 2018. 154: p. 27-37.
21. Cardoso, S., Mourão, Z., Pinho, C., Analysis of the thermal performance of an uncovered 1-hectare solar pond in Benguela, Angola. Case Studies in Thermal Engineering, 2021. 27: p.101254.
22. Namin, A.S., H. Rostamzadeh, and P. Nourani, *Thermodynamic and thermoeconomic analysis of three cascade power plants coupled with RO desalination unit, driven by a salinity-gradient solar pond.* Thermal Science and Engineering Progress, 2020. **18**: p. 100562.
23. Rostamzadeh., H., Nourani, P., Investigating potential benefits of a salinity gradient solar pond for ejector refrigeration cycle coupled with a thermoelectric generator. Energy, 2019. 172: p. 675-690.
24. Ziapour, B.M., Shokrnia, M., Naseri, M., Comparatively study between single-phase and two-phase modes of energy extraction in a salinity-gradient solar pond power plant. Energy, 2016. 111: p. 126-136.
25. Ziapour, B.M., Shokrnia, M., Exergoeconomic analysis of the salinity-gradient solar pond power plants using two-phase closed thermosyphon: A comparative study. Applied Thermal Engineering, 2017. 115: p. 123-133.
26. Erden, M., Karakilcik, M., Dincer, I., Performance investigation of hydrogen production

by the flat-plate collectors assisted by a solar pond. International Journal of Hydrogen Energy, 2017. 42: p. 2522-2529.
27. Rostamzadeha, H., Namin, A.S., Nourani, P., Amidpour, M., Ghaebi, H., Feasibility investigation of a humidification-dehumidification (HDH) desalination system with thermoelectric generator operated by a salinity-gradient solar pond. Desalination, 2019. 462: p. 1-18.
28. Zeynali, A., Akbari, A., Khalilian, M., Investigation of the performance of modified organic Rankine cycles (ORCs) and modified trilateral flash cycles (TFCs) assisted by a solar pond. Solar Energy, 2019. 182: p. 361-381.
29. Bernad, F., Casas, S., Gibert, O., Akbarzadeh, A., Cortina, J.L., Valderrama, C., 2013. Salinity gradient solar pond: Validation and simulation model. Sol. Energy 98, 366–374. doi:10.1016/j.solener.2013.10.004
30. Bryant, H. and I. Colbeck, *A solar pond for London?* Solar Energy, 1977. **19**(3): p. 321-322.
31. Green, D.W. and M.Z. Southard, *Perry's chemical engineers' handbook*. 2019: McGraw-Hill Education.
32. Ramires, M.L., et al., *Thermal conductivity of aqueous sodium chloride solutions.* Journal of Chemical and Engineering Data, 1994. **39**(1): p. 186-190.
33. Date, A., et al., *Heat extraction from non-convective and lower convective zones of the solar pond: a transient study.* Solar Energy, 2013. **97**: p. 517-528.
34. Fitzsimons, L., et al., *Modelling the activity of seawater and implications for desalination exergy analyses.* 2012.
35. Abdullah, A., et al., *Measurements of the performance of the experimental salt-gradient solar pond at Makkah one year after commissioning.* Solar Energy, 2017. **150**: p. 212-219.
36. Andrews, J. and A. Akbarzadeh, *Enhancing the thermal efficiency of solar ponds by extracting heat from the gradient layer.* Solar Energy, 2005. **78**(6): p. 704-716.
37. Karakilcik, M., I. Dincer, and M.A. Rosen, *Performance investigation of a solar pond.* Applied Thermal Engineering, 2006. **26**(7): p. 727-735.
38. Querol, E., B. Gonzalez-Regueral, and J.L. Perez-Benedito, *Exergetic Cost*, in *Practical Approach to Exergy and Thermoeconomic Analyses of Industrial Processes*. 2013, Springer. p. 39-62.
39. de Oliveira Junior, S., *Exergy: production, cost and renewability*. 2012: Springer Science & Business Media.
40. Kazim, A., *Exergoeconomic analysis of a PEM fuel cell at various operating conditions.* Energy Conversion and Management, 2005. **46**(7-8): p. 1073-1081.
41. *Annual Energy Outlook 2017 with projections to 2050.* EIA, 2018. **44**: p. 1-64.
42. Valderrama, C., J.L. Cortina, and A. Akbarzadeh, *Solar Ponds*, in *Storing Energy*. 2016, Elsevier. p. 273-289.